Uncertainties in the Magnetic Field of the Milky Way

Michael Unger[1] and Glennys R. Farrar[2]

[1]Institute for Nuclear Physics, Karlsruhe Institute of Technology
[2]Center for Cosmology and Particle Physics, New York University

Introduction

In this work we investigate uncertainties in the modeling of the global structure of the Galactic magnetic field (GMF). The starting point of the analysis is the model of Jannsson & Farrar (2012) [1, 2] in which the GMF is described by three divergence-free large-scale regular components and two components for the random field:

- regular spiral disk
- toroidal halo
- poloidal halo ("X-field")
- random spiral
- random halo

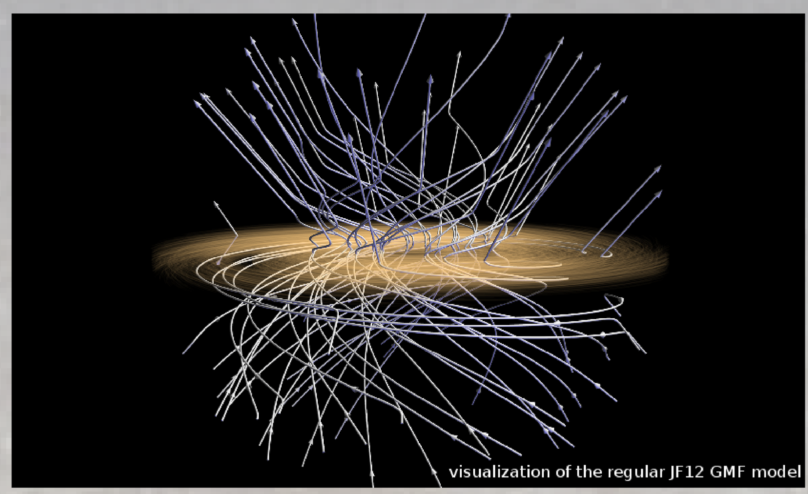

The 22+14 parameters of the regular and random magnetic field are constrained by multi-frequency radio observations of the Faraday rotation of extragalactic radio sources and measurements of the polarized and total Galactic synchrotron emission.

Data Analysis

The parameters of the different GMF models are optimized by minimizing the variance-weighted pixel-by-pixel difference between the predicted and measured observables. The following observables are calculated with the RUQI package:

- **Rotation measures (RMs)**: line-of-sight integral of the longitudinal magnetic field, weighted with the density of thermal electrons of the warm ionized medium of the Galaxy.
- **Polarized synchrotron intensity**: line of sight integral of the ordered component of the transverse magnetic field strength, weighted by the density of cosmic-ray electrons. The direction of the transverse magnetic field component can be inferred from the Stokes parameters Q and U.
- **Total (polarized and unpolarized) synchrotron intensity**: line-of-sight integral depending on the product of the cosmic-ray electron density and total transverse magnetic field strength (coherent and random).

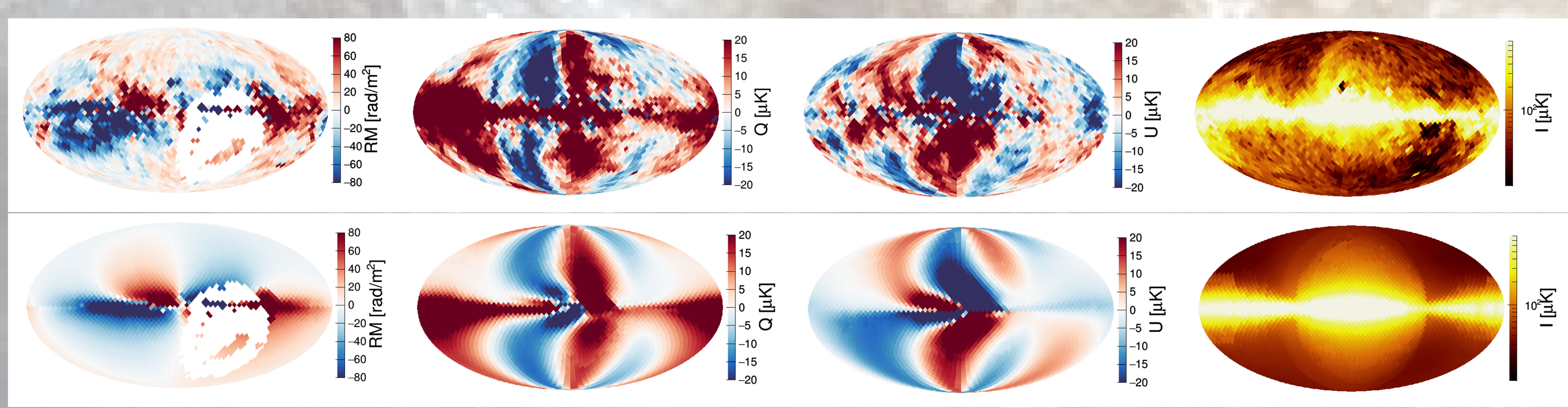

Figure 1: Measured (top) and simulated (bottom) sky maps of rotation measures (top), polarized synchrotron emission (Stokes Q and U parameters in the two middle panels) and total synchrotron intensity (bottom). The synchrotron data are from [3] and the GMF model is JF12 [1, 2].

Parameterizations

Several alternatives to the parameterizations of the coherent field used in the JF12 model were tested. All these alternatives are divergence-free, like the original functional forms.

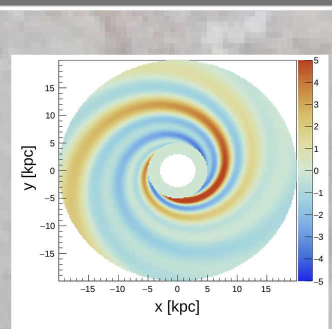

- poloidal X-field from [4]
- symmetric toroidal field
- Galactic warp
- smooth spiral field with free pitch angle
- twisted X-field

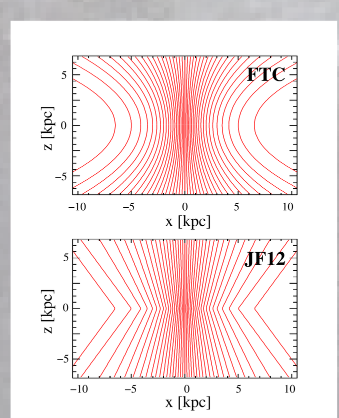

Synchrotron Data Products

Different interpretations of the microwave emission signals were tested: the 7-year WMAP synchrotron maps [3], as originally used in JF12, the 9-year final WMAP synchrotron products and the Planck 2015 data release [5]. These products differ in the constraints applied to the measured Galactic microwave emission data to extract the synchrotron component, most notably the treatment of the anomalous microwave emission.

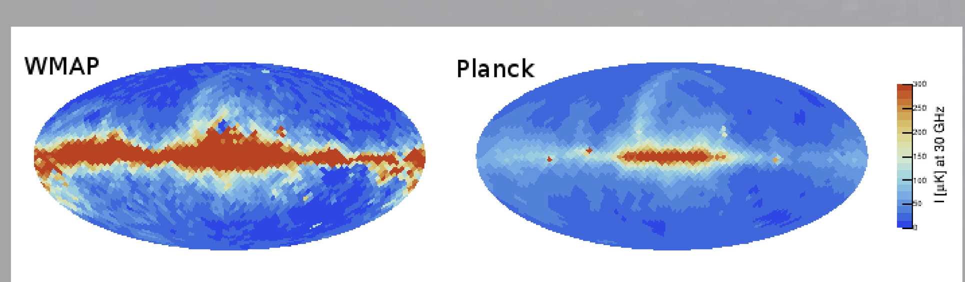

Thermal Electrons

We tested the impact of two different models for the thermal electron densities on the calculation of rotation measures: NE2001 [6], with the updated scale height of the thick disk from [7], and YMW17 [8]. While the newer YMW17 model relies on more dispersion measures from pulsars with measured distances, the more important difference between the two models lies in their particular parametric choices for the model components, such as the thickness and pitch angles of the spiral arms.

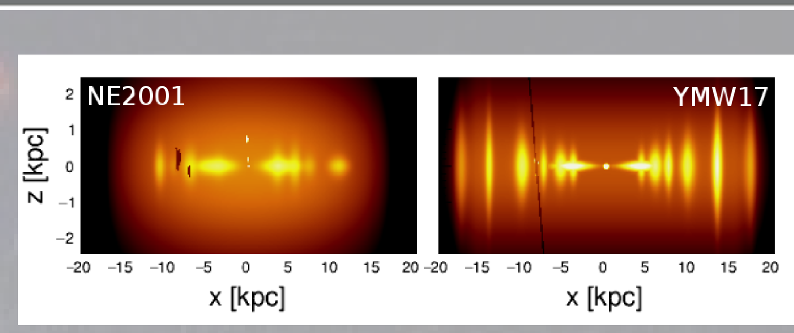

Cosmic-ray Electrons

The density and spectrum of cosmic-ray electrons depends in two ways on the Galactic magnetic field: Firstly, the GMF determines the diffusion of the electrons from their sources through the Galaxy and, secondly, synchrotron losses at high electron energies is the main cause of electron cooling.

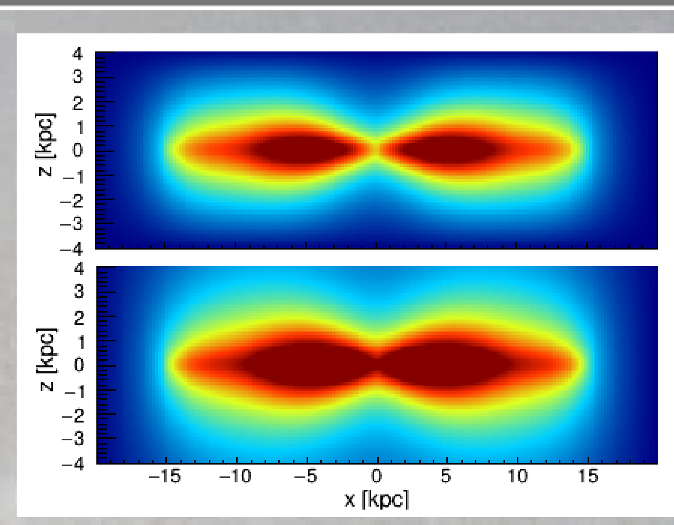

We tested the three variants of the cosmic-ray electron densities used in [9], which are updated versions of the calculations described in [10] and [11]. Two of them use a vertical extent of the diffusion volume of 4 kpc, whereas for variation *s* the height of the diffusion volume is 10 kpc.

Summary of Model Variations

	id	disk model	toroidal model	poloidal model	thermal electrons	cosmic-ray electrons	synchrotron data product	misc.	χ^2/ndf
Parametric models	a	JF	JF	JF	NE2001	GP_{JF}	WMAP7	-	1.10
	b	JF	JF	FTC	NE2001	GP_{JF}	WMAP7	-	1.09
	c	JF	JFsym	FTC	NE2001	GP_{JF}	WMAP7	-	1.11
	d	JF	JFsym	FTC	NE2001	GP_{JF}	WMAP7	warp	1.11
	e	UF	JFsym	FTC	NE2001	GP_{JF}	WMAP7	-	1.09
	f	UF	UFa		NE2001	GP_{JF}	WMAP7	-	1.14
	g	UF	UFb		NE2001	GP_{JF}	WMAP7	-	1.09
Synchrotron products	h	JF	JFsym	FTC	NE2001	GP_{JF}	WMAP9base	-	$1.22^\dagger$
	i	JF	JFsym	FTC	NE2001	GP_{JF}	WMAP9sdc	-	$1.24^\dagger$
	j	JF	JFsym	FTC	NE2001	GP_{JF}	WMAP9fs	-	$1.11^\dagger$
	k	JF	JFsym	FTC	NE2001	GP_{JF}	WMAP9fss	-	$1.22^\dagger$
	l	JF	JFsym	FTC	NE2001	GP_{JF}	Planck15	-	$0.78^\dagger$
Thermal electrons	m	JF	JFsym	FTC	YMW17	GP_{JF}	WMAP7	-	1.21
	n	UF	JFsym	FTC	YMW17	GP_{JF}	WMAP7	-	1.14
	o	JF	JF	FTC	NE2001	GP_{JF}	WMAP7	$\kappa = -1$	1.05^*
	p	JF	JF	FTC	NE2001	GP_{JF}	WMAP7	$\kappa = +1$	1.05^*
	q	JF	JFsym	FTC	NE2001	GP_{JF}	WMAP7	HIM	1.12
Cosmic-ray electrons	r	JF	JFsym	FTC	NE2001	O13a	WMAP7	-	1.13
	s	JF	JFsym	FTC	NE2001	O13b	WMAP7	-	1.12
	t	JF	JFsym	FTC	NE2001	S10	WMAP7	-	1.13

Table 1: List of model variations investigated. The original JF12 model corresponds to the first row (model a) and the reference model is given in the third row (model 3). The goodness of fit for describing the RM, Q and U data is given in the last column with the exception for the combined fits of coherent and random field (marked with a *), where the χ^2 also includes the contribution from the total intensity I. The χ^2s of the fits with different synchrotron data products (marked with a †) used different weights in the fits derived from these products.

Application to Charged Particle Astronomy

We performed a backtracking of charged particles through each of the GMF models listed in the Table above. In the absence of further input to select among or discard some of these models, the variation of the results gives a lower limit on the uncertainty of the inferred arrival direction of extragalactic cosmic rays at the edge of the Galaxy. The backtracked directions for different regions of the sky and particle rigidities are shown in the figure below.

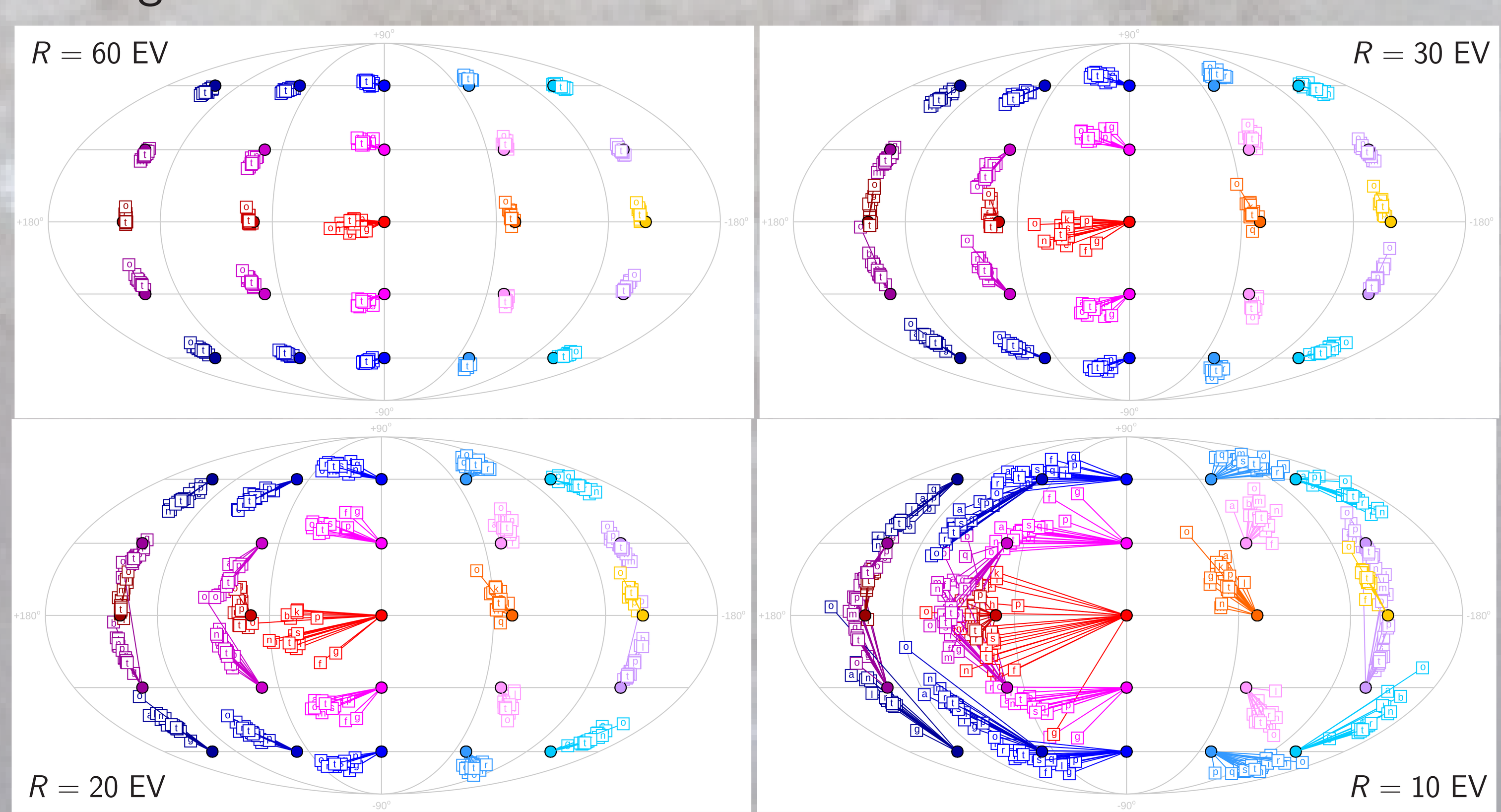

Figure 2: Backtracking of charged particles at different rigidities from a regular grid of initial directions (dots) through different models of the coherent GMF. The resulting directions outside of the Galaxy are denoted by squares and the letters correspond to the models listed in Table 1. The sky maps are in Galactic coordinates and the particle rigidities indicated in corners of each panel.

References

[1] R. Jansson and G. R. Farrar *ApJ* **757** (2012) 14.

[2] R. Jansson and G. R. Farrar *ApJ* **761** (2012) L11.

[3] B. Gold *et al.*, [WMAP Collab.] *ApJS* **192** (2011) 15.

[4] K. Ferrière and P. Terral *A&A* **561** (2014) A100.

[5] R. Adam *et al.*, [Planck Collab.] *A&A* **594** (2016) A10.

[6] J. M. Cordes and T. J. W. Lazio *arXiv:0207156 [astro-ph]* (2002) .

[7] B. M. Gaensler, G. J. Madsen, S. Chatterjee, and S. A. Mao *PASA* **25** (2008) 184–200.

[8] J. M. Yao, R. N. Manchester, and N. Wang *ApJ* **835** (2017) 29.

[9] R. Adam *et al.*, [Planck Collab.] *A&A* **596** (2016) A103.

[10] A. W. Strong *et al.* *ApJ* **722** (2010) L58–L63.

[11] E. Orlando and A. Strong *MNRAS* **436** (2013) 2127–2142.

michael.unger@kit.edu, gf25@nyu.edu